Effective potential study of the rotational excitation of HD by collision with H2

Shihl Chu

Citation: The Journal of Chemical Physics **62**, 4089 (1975); doi: 10.1063/1.430285
View online: http://dx.doi.org/10.1063/1.430285
View Table of Contents: http://scitation.aip.org/content/aip/journal/jcp/62/10?ver=pdfcov
Published by the AIP Publishing

Effective potential study of the rotational excitation of HD by collision with H_2

Shih-I Chu

Joint Institute for Laboratory Astrophysics, University of Colorado and National Bureau of Standards, Boulder, Colorado 80302

(Received 14 January 1975)

The effective potential formalism of Rabitz is extended to a general potential expressed in terms of relative or body-fixed coordinates and applied to the study of the H_2–HD rotationally inelastic collisions. The H_2 and HD molecules are treated as rigid rotors and their interaction potential is derived from the H_2–H_2 potential. Long-range quadrupole–dipole and quadrupole–quadrupole interactions are also considered. Quantum-mechanical close-coupling calculations for three-dimensional collisions of para-H_2 and ortho-H_2 with HD are performed up to $E = 0.20$ eV. The general features of the rotational excitation cross sections of HD are examined and their sensitivity to certain aspects of the potential are analyzed. In particular, the different roles of the short- and long-range anisotropies are illustrated. It is found that the degree of anisotropy is meaningful only in relation to the magnitude of the "effectively" spherically symmetric part of potential. The rate constants for pure rotational transitions of HD are presented in the temperature range of 5 to 800 °K. The relation of these results to the quantitative interpretation of the thermal balance of interstellar clouds is pointed out. We have also calculated the rotational relaxation times for the lowest two levels of HD, which could be examined and compared with future sound absorption experiments to assess the accuracy of the H_2–HD interaction potential.

I. INTRODUCTION

In the last few years, a number of efficient though approximate quantum-mechanical methods[1–3] have been developed, aimed at overcoming the computational difficulties which arise in the conventional formulation of the molecule–molecule collision problem. In particular, Rabitz[1] has developed an effective potential method [also called the effective close-coupling (ECC) method[4]] which averages the interaction potential over the initial and final angular momentum projections. As a result, the rotational angular momentum **j** and the orbital angular momentum **l** are decoupled and the number of coupled equations is greatly reduced. For a scattering calculation involving N internal states, the ECC formalism needs the solution of only N coupled equations rather than N^2 as would be required in the conventional close-coupling formalism. This represents a significant reduction in the computational effort. The ECC method has been applied successfully by Zarur and Rabitz[5,6] to He–H_2 and H_2–H_2 rotational inelastic collisions. It has also been adopted by Chu and Dalgarno[4,7] in their studies of the rotational inelastic collision of H + CO and the angular distribution of the rotational elastic collision of H + H_2. More recently, Rabitz and Zarur[8] and Alexander[9] have extended the ECC method to studies of He–H_2 rotational–vibrational inelastic scattering.

The effective close-coupling method, while providing an efficient and reasonable computational scheme for some of the collision problems, is not without limitations. For example, Chu[10] found that it is not reliable when applied to H–CS and H_2–CO collisions. Recently, Green[11] also found that the ECC method is not adequate for describing the He–HCN collision. In a recent paper, Chu and Dalgarno[12] examined the range of applicability of several simplified quantum-mechanical scattering approaches, including the ECC one. Their main conclusions about the ECC method are that it is likely to be unreliable for collision systems with a strong repulsive anisotropy, and that it requires some modification of the original detailed-balance relationship.[1]

In this paper, we apply the ECC formalism to the study of rotationally inelastic collisions between H_2 and HD. The repulsive anisotropy for this system is not very strong, and the ECC formalism should work reasonably well. The study is motivated by the importance of the collision process in interstellar clouds. The molecules HD and CO are the most abundant interstellar molecules, second only to H_2, and the efficiency with which the rotational levels of HD and CO are excited by impact with molecular hydrogen is critical to the quantitative determination of the thermal balance of molecular clouds and to their evolution towards the formation of protostars. Information about the H_2–CO collision has recently been provided by Green and Thaddeus.[13] But the corresponding information about the H_2–HD collision is lacking. The rotational excitation of HD by impact with He has been studied by a number of groups.[14–16] The HD–HD system has also been treated by Takayanagi[17] using the modified wavenumber approximation. The study of H_2–HD collisions is of interest in connection with the determination of the interstellar D/H ratio,[18] which is an important parameter in the study of the evolution of the Galaxy.

In Sec. II, the effective potential formalism for molecule–molecule collision is presented for a general potential expressed in terms of body-fixed coordinates rather than space-fixed coordinates as used by Rabitz.[1] The transformation between these two sets of effective interaction potentials is explicitly worked out. The derivations of the coupled equations and cross-section expressions are also briefly reviewed. The interaction potential between H_2 and HD is derived from the H_2–H_2 potential and discussed in Sec. III. Long-range quadrupole–dipole and quadrupole-quadrupole interactions are

also considered. Section IV discusses the method of solving the coupled equations and the choice of basis set. Section V presents the results of scattering calculations. The general features of these cross sections and their sensitivity to the potential are analyzed. The differences between para-H_2 and ortho-H_2 in collision with HD are also examined. In Sec. VI, the rate constants for pure HD rotational transitions are provided. Finally, in Sec. VII, we present the rotational relaxation times for the lowest two levels of HD. These results are useful for future comparison with sound absorption experiments and can be used to test and improve the accuracy of the H_2–HD potential.

II. THE EFFECTIVE POTENTIAL FORMULATION OF MOLECULE-MOLECULE COLLISIONS

Consider the collisions of two linear rigid rotating molecules. The Hamiltonian for the scattering system can be written as

$$H = T + H_0(\text{int}) + V \quad , \tag{1}$$

where T is the kinetic energy operator, $H_0(\text{int})$ is the rotational Hamiltonian for the unperturbed molecules, and V is the intermolecular potential. In his original derivation, Rabitz[1] assumed that the intermolecular potential V can be expanded in spherical harmonics:

$$V = \sum_{l_1 l_2 l} \sum_{m_1 m_2 m} A_{l_1 l_2 l}(R) \langle l_1 m_1 l_2 m_2 | l_1 l_2 l m \rangle \times Y_{l_1 m_1}(\hat{\Omega}_1) Y_{l_2 m_2}(\hat{\Omega}_2) Y^*_{lm}(\hat{R}) \quad , \tag{2}$$

where $\langle \cdots | \cdots \rangle$ is a Clebsch–Gordan coefficient, and the unit vectors $\hat{\Omega}_1$, $\hat{\Omega}_2$, and $\hat{R}$ are, respectively, the orientation of molecule 1 and 2 and the vector **R** between the centers of mass of the two molecules. All the angles are measured with respect to a space-fixed coordinate system. This potential [Eq. (2)] is quite general in form because the radial coefficients $A_{l_1 l_2 l}(R)$ have not been specified. These coefficients are known in detail for very few systems. The only exception is the electric long-range multipolar part of the potential, where $A_{l_1 l_2 l}(R)$ is known to have the form[19]

$$A_{l_1 l_2 l}(R) = \left[\frac{4\pi(-1)^{l_2}}{(2l+1)}\right]\left[\frac{4\pi(2l+1)!}{(2l_1+1)!(2l_2+1)!}\right]^{1/2}\left(\frac{Q_{l_1} Q_{l_2}}{R^{l+1}}\right) \quad , \tag{3}$$

where $l_1 + l_2 = l$ and Q_{l_i} is the l_ith multipole moment on molecule $i = 1, 2$. For short-range potentials, it is usually more convenient[20] to expand the potential in terms of the body-fixed coordinates $\omega_1 = (\theta_1, \phi_1)$, $\omega_2 = (\theta_2, \phi_2)$, and $\hat{\Omega}_1 \cdot \hat{\Omega}_2$, shown in Fig. 1. Complete sets of functions of these angles for two linear molecules are given by the Legendre polynomials $P_{l_1}(\cos\theta_1)$, $P_{l_2}(\cos\theta_2)$, and $P_l[\cos(\hat{\Omega}_1 \cdot \hat{\Omega}_2)]$, respectively. The potential V in body-fixed coordinates is then given by

$$V = \sum_{l_1 l_2 l} v_{l_1 l_2 l}(R) P_{l_1}(\cos\theta_1) P_{l_2}(\cos\theta_2) P_l(\cos\chi_{12}) \quad , \tag{4}$$

where the body-fixed coordinates are related to the space-fixed coordinates by $\theta_1 = \cos^{-1}(\hat{\Omega}_1 \circ \hat{R})$, $\theta_2 = \cos^{-1}(\hat{\Omega}_2 \cdot \hat{R})$, and $\chi_{12} = \cos^{-1}(\hat{\Omega}_1 \circ \hat{\Omega}_2)$. These two expansion forms, Eqs. (2) and (4), are equivalent and they are related by an angular momentum transformation. In order to extend the usefulness of the effective potential method, we derive the effective potential based on the expansion form given in Eq. (4).

The rotor states $|j_1 m_1 j_2 m_2\rangle$ are eigenstates of $H_0(\text{int})$ with eigenvalues $(\epsilon_{j_1} + \epsilon_{j_2})$ such that

$$\langle j_1 m_1 j_2 m_2 | H_0(\text{int}) | j_1' m_1' j_2' m_2' \rangle = (\epsilon_{j_1} + \epsilon_{j_2}) \delta_{j_1 j_1'} \delta_{j_2 j_2'} \delta_{m_1 m_1'} \delta_{m_2 m_2'} \quad . \tag{5}$$

The potential in Eq. (4) in the representation of eigenstates of $H_0(\text{int})$ can be written as

$$\langle j_1 m_1 j_2 m_2 | V | j_1' m_1' j_2' m_2' \rangle = \sum_{l_1 l_2 l} \sum_{l' l'' \lambda} A^{l' l'' \lambda}_{l_1 l_2 l}(R) \langle j_1 j_2 || T_{l' m' \lambda} || j_1' j_2' \rangle F\begin{pmatrix} j_1 & j_2 & j_1' & j_2' \\ m_1 & m_2 & m_1' & m_2' \end{pmatrix} \hat{R} \quad , \tag{6}$$

where all the angular factors and the magnetic quantum numbers have been absorbed into the function F. The effective potential method[1] seeks an effective potential that will couple j_1 and j_2 to j_1' and j_2' regardless of orientation effects. The form of Eq. (6) implies that the product $A^{l' l'' \lambda}_{l_1 l_2 l}(R) \langle j_1 j_2 || T_{l' m' \lambda} || j_1' j_2' \rangle$ might serve the dominant role of the effective potential. However, the presence of the angular function F requires additional consideration.

To find suitable expressions for A, $\langle \| T \| \rangle$, and F in Eq. (6), we have first to express $P_{l_1}(\cos\theta_1) P_{l_2}(\cos\theta_2) P_l(\cos\chi_{12})$ in terms of the product of spherical harmonics, $Y_{l' m'}(\hat{\Omega}_1) Y_{l'' m''}(\hat{\Omega}_2) Y^*_{\lambda\mu}(\hat{R})$. Now

$$P_{l_1}(\cos\theta_1) P_{l_2}(\cos\theta_2) P_l(\cos\chi_{12}) = \sum_{\lambda = |l_1 - l_2|}^{l_1 + l_2} \langle l_1 0 l_2 0 | l_1 l_2 \lambda 0 \rangle [C^{(l)}(\hat{1}) \cdot C^{(l)}(\hat{2})] \{[C^{(l_1)}(\hat{1}) \times C^{(l_2)}(\hat{2})]^{(\lambda)} \cdot C^{(\lambda)}(\hat{R})\} \quad , \tag{7}$$

where $C^{(p)}(\hat{1})$, $C^{(q)}(\hat{2})$, and $C^{(s)}(\hat{R})$ are, respectively, the normalized spherical tensors for $\hat{\Omega}_1$ (of rank p), $\hat{\Omega}_2$ (of rank q), and $\hat{R}$ (of rank s). Using the phase convention of Brink and Satchler,[21] we have

$$C^{(l)}(\hat{1}) \circ C^{(l)}(\hat{2}) = \sum_q (-1)^q C^{(l)}_q(\hat{1}) C^{(l)}_{-q}(\hat{2}) \quad , \tag{8a}$$

$$[C^{(l_1)}(\hat{1}) \times C^{(l_2)}(\hat{2})]^{(\lambda)} \cdot C^{(\lambda)}(\hat{R}) = \sum_\mu (-1)^\mu [C^{(l_1)}(\hat{1}) \times C^{(l_2)}(\hat{2})]^{(\lambda)}_\mu C^{(\lambda)}_{-\mu}(\hat{R}) \quad , \tag{8b}$$

and

$$[C^{(l_1)}(\hat{1}) \times C^{(l_2)}(\hat{2})]^{(\lambda)}_{\mu} = \sum_{\mu_1} \sum_{\mu_2} \langle l_1 \mu_1 l_2 \mu_2 | l_1 l_2 \lambda \mu \rangle C^{(l_1)}_{\mu_1}(\hat{1}) C^{(l_2)}_{\mu_2}(\hat{2}) \ , \tag{8c}$$

where

$$C^{(l)}_q \equiv \left(\frac{4\pi}{2l+1}\right)^{1/2} Y_{lq} \ , \quad \text{etc.}$$

Substituting Eqs. (8a)–(8c) into Eq. (7), we obtain

$$P_{l_1}(\cos\theta_1) P_{l_2}(\cos\theta_2) P_l(\cos\chi_{12}) = \sum_{\lambda=|l_1-l_2|}^{l_1+l_2} \left[\frac{2\lambda+1}{(2l+1)^2(2l_1+1)(2l_2+1)}\right]^{1/2} (4\pi)^{5/2} \begin{pmatrix} l_1 & l_2 & \lambda \\ 0 & 0 & 0 \end{pmatrix}$$

$$\times \sum_{q=-l}^{l} \sum_{\mu=-\lambda}^{\lambda} \sum_{\mu_1=-l_1}^{l_1} \sum_{\mu_2=-l_2}^{l_2} \begin{pmatrix} l_1 & l_2 & \lambda \\ \mu_1 & \mu_2 & -\mu \end{pmatrix} Y_{lq}(\hat{\Omega}_1) Y_{l_1\mu_1}(\hat{\Omega}_1) Y^*_{lq}(\hat{\Omega}_2) Y_{l_2\mu_2}(\hat{\Omega}_2) Y_{\lambda,-\mu}(\hat{R}) \ , \tag{9}$$

where

$$\begin{pmatrix} \cdot & \cdot & \cdot \\ \cdot & \cdot & \cdot \end{pmatrix}$$

is the $3j$ symbol. Using the addition relations for spherical harmonics,[21]

$$Y_{lq}(\hat{\Omega}_1) Y_{l_1\mu_1}(\hat{\Omega}_1) = (-1)^{q+\mu_1} \sum_{l'm'} \left(\frac{[l][l_1][l']}{4\pi}\right)^{1/2} \begin{pmatrix} l & l_1 & l' \\ 0 & 0 & 0 \end{pmatrix} \begin{pmatrix} l & l_1 & l' \\ -q & -\mu_1 & m' \end{pmatrix} Y_{l'm'}(\hat{\Omega}_1) \ ,$$

and

$$Y^*_{lq}(\hat{\Omega}_2) Y_{l_2\mu_2}(\hat{\Omega}_2) = (-1)^{\mu_2} \sum_{l''m''} \left(\frac{[l][l_2][l'']}{4\pi}\right)^{1/2} \begin{pmatrix} l & l_2 & l'' \\ 0 & 0 & 0 \end{pmatrix} \begin{pmatrix} l & l_2 & l'' \\ q & -\mu_2 & m'' \end{pmatrix} Y_{l''m''}(\hat{\Omega}_2) \ ,$$

where $[l] \equiv 2l+1$, etc., Eq. (9) becomes

$$P_{l_1}(\cos\theta_1) P_{l_2}(\cos\theta_2) P_l(\cos\chi_{12}) = \sum_{\lambda=|l_1-l_2|}^{l_1+l_2} (4\pi)^{3/2} [\lambda]^{1/2} \begin{pmatrix} l_1 & l_2 & \lambda \\ 0 & 0 & 0 \end{pmatrix} \sum_{\mu} \sum_{l'} \sum_{m'} \sum_{l''} \sum_{m''} ([l'][l''])^{1/2} \begin{pmatrix} l & l_1 & l' \\ 0 & 0 & 0 \end{pmatrix} \begin{pmatrix} l & l_2 & l'' \\ 0 & 0 & 0 \end{pmatrix}$$

$$\times \sum_{q} \sum_{\mu_1} \sum_{\mu_2} (-1)^{q+\mu_1+\mu_2} \begin{pmatrix} l_1 & l_2 & \lambda \\ \mu_1 & \mu_2 & -\mu \end{pmatrix} \begin{pmatrix} l & l_1 & l' \\ -q & -\mu_1 & m' \end{pmatrix} \begin{pmatrix} l & l_2 & l'' \\ q & -\mu_2 & m'' \end{pmatrix} Y_{l'm'}(\hat{\Omega}_1) Y_{l''m''}(\hat{\Omega}_2) Y_{\lambda,-\mu}(\hat{R}) \ . \tag{10}$$

Next from the contraction formula,[21]

$$\sum_{\delta\epsilon\phi} \begin{pmatrix} d & e & c \\ -\delta & \epsilon & \gamma \end{pmatrix} \begin{pmatrix} e & f & a \\ -\epsilon & \phi & \alpha \end{pmatrix} \begin{pmatrix} f & d & b \\ -\phi & \delta & \beta \end{pmatrix} (-1)^{d+e+f-\delta-\epsilon-\phi} = \begin{Bmatrix} a & b & c \\ d & e & f \end{Bmatrix} \begin{pmatrix} a & b & c \\ \alpha & \beta & \gamma \end{pmatrix} \ , \tag{11}$$

the third summations on the rhs of Eq. (10) can be rewritten as

$$\sum_{q} \sum_{\mu_1} \sum_{\mu_2} (-1)^{q+\mu_1+\mu_2} \begin{pmatrix} l_1 & l_2 & \lambda \\ \mu_1 & \mu_2 & -\mu \end{pmatrix} \begin{pmatrix} l & l_1 & l' \\ -q & -\mu_1 & m' \end{pmatrix} \begin{pmatrix} l & l_2 & l'' \\ q & -\mu_2 & m'' \end{pmatrix} = (-1)^{l_1+l'+\lambda} \begin{Bmatrix} l'' & l' & \lambda \\ l_1 & l_2 & l \end{Bmatrix} \begin{pmatrix} l' & l'' & \lambda \\ m' & m'' & -\mu \end{pmatrix} \ . \tag{12}$$

Substituting Eq. (12) into Eq. (10), we finally arrive at the desired expression for the angular momentum transformation between body-fixed and space-fixed coordinates,[22]

$$P_{l_1}(\cos\theta_1) P_{l_2}(\cos\theta_2) P_l(\cos\chi_{12}) = \sum_{\lambda} \sum_{l'} \sum_{l''} \sum_{\mu} \sum_{m'} \sum_{m''} (-1)^{l_1+l''+\lambda+\mu} (4\pi)^{3/2} ([\lambda][l'][l''])^{1/2}$$

$$\times \begin{pmatrix} l_1 & l_2 & \lambda \\ 0 & 0 & 0 \end{pmatrix} \begin{pmatrix} l & l_1 & l' \\ 0 & 0 & 0 \end{pmatrix} \begin{pmatrix} l & l_2 & l'' \\ 0 & 0 & 0 \end{pmatrix} \begin{Bmatrix} l'' & l' & \lambda \\ l_1 & l_2 & l \end{Bmatrix} \begin{pmatrix} l' & l'' & \lambda \\ m' & m'' & -\mu \end{pmatrix} Y_{l'm'}(\hat{\Omega}_1) Y_{l''m''}(\hat{\Omega}_2) Y^*_{\lambda\mu}(\hat{R}) \ . \tag{13}$$

Using this result, the matrix elements for the potential given in Eq. (6) can now be evaluated explicitly as

$$\langle j_1 m_1 j_2 m_2 | V | j_1' m_1' j_2' m_2' \rangle = \sum_{l_1 l_2 l} v_{l_1 l_2 l}(R) \sum_{l' l'' \lambda} \sum_{m' m'' \mu} (-1)^{l_1+l'+m_1+m_2+\lambda+\mu} (4\pi)^{1/2}$$

$$\times ([\lambda][l']^2[l'']^2[j_1][j_1'][j_2][j_2'])^{1/2} \begin{pmatrix} l_1 & l_2 & \lambda \\ 0 & 0 & 0 \end{pmatrix} \begin{pmatrix} l & l_1 & l' \\ 0 & 0 & 0 \end{pmatrix} \begin{pmatrix} l & l_2 & l'' \\ 0 & 0 & 0 \end{pmatrix} \begin{Bmatrix} l'' & l' & \lambda \\ l_1 & l_2 & l \end{Bmatrix}$$

$$\times \begin{pmatrix} j_1 & l' & j_1' \\ 0 & 0 & 0 \end{pmatrix} \begin{pmatrix} j_2 & l'' & j_2' \\ 0 & 0 & 0 \end{pmatrix} \begin{pmatrix} l' & l'' & \lambda \\ m' & m'' & -\mu \end{pmatrix} \begin{pmatrix} j_1 & l' & j_1' \\ -m_1 & m' & m_1' \end{pmatrix} \begin{pmatrix} j_2 & l'' & j_2' \\ -m_2 & m'' & m_2' \end{pmatrix} Y^*_{\lambda\mu}(\hat{R}) \ , \tag{14}$$

where use has been made of the following formula[21]:

$$\langle j_1 m_1 | Y_{l'm'} | j_1' m_1' \rangle = (-1)^{m_1} \left(\frac{[j_1][l'][j_1']}{4\pi} \right)^{1/2} \begin{pmatrix} j_1 & l' & j_1' \\ 0 & 0 & 0 \end{pmatrix} \begin{pmatrix} j_1 & l' & j_1' \\ -m_1 & m' & m_1' \end{pmatrix} ,$$

etc. Comparing Eqs. (14) and (6), and using the following constraints for $\langle \| T_{l'l''\lambda} \| \rangle$ and F, namely,

$$\langle j_1 j_2 \| T_{l'l''\lambda} \| j_1' j_2' \rangle = \langle j_1' j_2' \| T_{l'l''\lambda} \| j_1 j_2 \rangle , \tag{15}$$

$$F^* \begin{pmatrix} j_1' & j_2' & j_1 & j_2 \\ m_1' & m_2' & m_1 & m_2 \end{pmatrix} \hat{R} = F \begin{pmatrix} j_1 & j_2 & j_1' & j_2' \\ m_1 & m_2 & m_1' & m_2' \end{pmatrix} \hat{R} , \tag{16}$$

and

$$\sum_{m's} \left| F \begin{pmatrix} j_1 & j_2 & j_1' & j_2' \\ m_1 & m_2 & m_1' & m_2' \end{pmatrix} \hat{R} \right|^2 = 1 , \tag{17}$$

we obtain for A, $\langle \| T \| \rangle$, and F,

$$A_{l_1 l_2 l}^{l' l'' \lambda}(R) = (4\pi)^{3/2} ([l'][l''])^{1/2} (-1)^l \begin{pmatrix} l_1 & l_2 & \lambda \\ 0 & 0 & 0 \end{pmatrix} \begin{pmatrix} l & l_1 & l' \\ 0 & 0 & 0 \end{pmatrix} \begin{pmatrix} l_2 & l & l'' \\ 0 & 0 & 0 \end{pmatrix} \begin{Bmatrix} l'' & l' & \lambda \\ l_1 & l_2 & l \end{Bmatrix} v_{l_1 l_2 l}(R) , \tag{18}$$

$$\langle j_1 j_2 \| T_{l'l''\lambda} \| j_1' j_2' \rangle = ([\lambda][j_1][j_2][j_1'][j_2'])^{1/2} \begin{pmatrix} j_1 & l' & j_1' \\ 0 & 0 & 0 \end{pmatrix} \begin{pmatrix} j_2 & l'' & j_2' \\ 0 & 0 & 0 \end{pmatrix} , \tag{19}$$

and

$$F \begin{pmatrix} j_1 & j_2 & j_1' & j_2' \\ m_1 & m_2 & m_1' & m_2' \end{pmatrix} \hat{R} = (4\pi [l'][l''])^{1/2} \sum_{m' m'' \mu} (-1)^{m_1 + m_2' + \lambda + \mu} Y_{\lambda\mu}^*(\hat{R}) \begin{pmatrix} l' & l'' & \lambda \\ m' & m'' & -\mu \end{pmatrix} \begin{pmatrix} j_1 & l' & j_1' \\ -m_1 & m' & m_1' \end{pmatrix} \begin{pmatrix} j_2 & l'' & j_2' \\ -m_2 & m'' & m_2' \end{pmatrix} . \tag{20}$$

The angular function F in Eq. (20) can be interpreted as a probability amplitude for the m-dependent couplings by a tensor of order λ when the molecules are oriented at angle $\hat{R}$ with respect to each other. The contraction of F^* with V [cf. Eq. (6)] will yield the sum over the products $A_{l_1 l_2 l}^{l' l'' \lambda}(R) \langle j_1 j_2 \| T_{l'l''\lambda} \| j_1' j_2' \rangle$, the latter being independent of the orientation effects. Thus, the effective operator Q^{eff} may be taken as

$$\langle j_1 j_2 | Q^{\text{eff}} | j_1' j_2' \rangle = \sum_{m's} G \begin{pmatrix} j_1 & j_2 & j_1' & j_2' \\ m_1 & m_2 & m_1' & m_2' \end{pmatrix} \hat{R} \langle j_1 m_1 j_2 m_2 | Q | j_1' m_1' j_2' m_2' \rangle , \tag{21}$$

where $Q = H_0(\text{int})$ or V, and G is a function that behaves like F^* and its appropriate form is to be determined.

The derivation of the function G is the essential part of the effective potential method and has been given in detail by Rabitz[1] in his original formulation. Here we simply remark that the functions G are subject to the following three constraints[1]:

(i) the spectrum of $H_0^{\text{eff}}(\text{int})$ should possess the same structure as $H_0(\text{int})$,

$$\langle j_1 j_2 | H_0^{\text{eff}}(\text{int}) | j_1' j_2' \rangle = (\epsilon_{j_1} + \epsilon_{j_2}) \delta_{j_1 j_1'} \delta_{j_2 j_2'} , \tag{22}$$

(ii) the effective Hamiltonian should be Hermitian,

$$\langle j_1 j_2 | H^{\text{eff}} | j_1' j_2' \rangle^* = \langle j_1' j_2' | H^{\text{eff}} | j_1 j_2 \rangle , \tag{23}$$

(iii) the function G should be physically meaningful. Using a general nth-order perturbation theory, Rabitz[1] chose the lowest order coupling term $G_1 (\sim F^*)$ as the effective representation of G. This choice is consistent with constraint (iii) in that V^{eff} retains the meaning of a potential. By further imposing constraints (i) and (ii), the function G is completely determined and the matrix elements of the effective Hamiltonian become

$$\langle j_1 j_2 | H^{\text{eff}} | j_1' j_2' \rangle = [-(\hbar^2/2\mu) \nabla_R^2 + \epsilon_{j_1} + \epsilon_{j_2}] \delta_{j_1 j_1'} \delta_{j_2 j_2'} + \langle j_1 j_2 | V^{\text{eff}}(R) | j_1' j_2' \rangle , \tag{24}$$

where μ is the reduced mass of the colliding system. If the potential V is expanded in terms of the body-fixed coordinates [Eq. (6)], then the matrix elements for the corresponding effective potential are found to be

$$\langle j_1 j_2 | V^{\text{eff}}(R) | j_1' j_2' \rangle = N e^{i\eta} \sum_{l_1 l_2 l} \sum_{l' l'' \lambda} A_{l_1 l_2 l}^{l' l'' \lambda}(R) \langle j_1 j_2 \| T_{l'l''\lambda} \| j_1' j_2' \rangle , \tag{25}$$

with

$$N = ([j_1][j_2][j_1'][j_2'])^{-1/4} , \tag{26a}$$

and

$$\eta = \tfrac{1}{2}\pi [| j_1 + j_2 - j_1' - j_2' | + j_1 + j_2 + j_1' + j_2'] . \tag{26b}$$

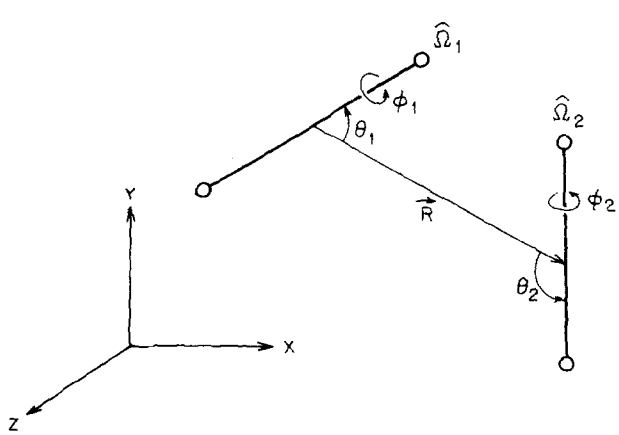

FIG. 1. Body-fixed coordinates for a pair of linear molecules. XYZ is a space fixed reference frame.

To solve the dynamical problem we expand the $j_1 j_2$ component of the total wavefunction for the relative motion of the system in the form

$$\psi_{j_1 j_2}(\mathbf{R}) = \frac{1}{R}\sum_{l=0}^{\infty} U^l_{j_1 j_2}(R) P_l(\cos\theta) \ , \tag{27}$$

where θ is the polar angle of **R**. Substituting Eq. (27) into the Schrödinger equation, $H^{\text{eff}}\psi = E\psi$, we obtain the set of coupled differential equations,

$$\left[\frac{d^2}{dR^2} - \frac{l(l+1)}{R^2} + k^2_{j_1 j_2}\right] U^l_{j_1 j_2}(R)$$

$$= \sum_{j_1' j_2'} \frac{2\mu}{\hbar^2} \langle j_1 j_2 | V^{\text{eff}}(R) | j_1' j_2' \rangle U^l_{j_1' j_2'}(R) \ , \tag{28}$$

where

$$k^2_{j_1 j_2} = (2\mu/\hbar^2)(E - \epsilon_{j_1} - \epsilon_{j_2}) \ , \tag{29}$$

E being the total collision energy. These close-coupled equations are to be solved for the functions $U^l_{j_1 j_2}(R)$ after truncation of the sum over $j_1' j_2'$ at some appropriate size. There exists a set of such equations for each value of the orbital angular momentum l, which essentially serves the same role as the total angular momentum J in the conventional close-coupling theory.

Asymptotically, the wavefunction $\psi_{j_1' j_2'}(R)$ becomes

$$\lim_{R\to\infty} \psi_{j_1' j_2'}(R) \sim [1/(2\pi)^{3/2}][\delta_{j_1 j_1'}\delta_{j_2 j_2'} \exp(ik_{j_1 j_2} R\cos\theta)$$

$$+ (1/R) f(j_1 j_2 \to j_1' j_2' | \theta) \exp(ik_{j_1' j_2'} R)] \ . \tag{30}$$

The scattering amplitude can be expanded in terms of Legendre polynomials as

$$f(j_1 j_2 \to j_1' j_2' | \theta) = \sum_{l=0}^{\infty} (2l+1) f_l(j_1 j_2 \to j_1' j_2') P_l(\cos\theta) \ . \tag{31}$$

Then it can be readily shown that the individual $f_l(j_1 j_2 \to j_1' j_2')$ is given by

$$f_l(j_1 j_2 \to j_1' j_2')$$

$$= \tfrac{1}{2} i [\delta_{j_1 j_1'}\delta_{j_2 j_2'} - S_l(j_1 j_2; j_1' j_2')]/(k_{j_1 j_2} k_{j_1' j_2'})^{1/2} \ , \tag{32}$$

where the effective partial S-matrix elements, $S_l(j_1 j_2; j_1' j_2')$, are obtained from the asymptotic form of the solutions to the coupled equations, Eqs. (28).

The effective differential cross section for a collision-induced transition from the initial state $|j_1 j_2\rangle$ to the final state $|j_1' j_2'\rangle$ is

$$\frac{d\sigma}{d\Omega}(j_1 j_2 \to j_1' j_2' | \theta)$$

$$= g(j_1 j_2; j_1' j_2') \frac{k_{j_1' j_2'}}{k_{j_1 j_2}} |f(j_1 j_2 \to j_1' j_2' | \theta)|^2 \ , \tag{33}$$

where g is a counting-of-states function[6] introduced to make the differential cross sections satisfy the detailed balance relation. The choice of g is, however, not unique but depends upon the nature of the intermolecular force and the energy range under consideration. For a system with weak repulsive anisotropy like H_2–HD, Chu and Dalgarno[12] found that the appropriate form for g is

$$g(j_1 j_2; j_1' j_2') = [(2j_1'+1)(2j_2'+1)/(2j_1+1)(2j_2+1)]^{1/2} \ , \tag{34}$$

as suggested by Zarur and Rabitz[6] in their H_2–H_2 studies. The total cross section is obtained by integrating $d\sigma/d\Omega$ over all angles:

$$\sigma(j_1 j_2 \to j_1' j_2') = \int d\Omega \frac{d\sigma}{d\Omega}(j_1 j_2 \to j_1' j_2' | \theta)$$

$$= \frac{\pi}{k^2_{j_1 j_2}} g(j_1 j_2; j_1' j_2')$$

$$\times \sum_{l=0}^{\infty} (2l+1) |\delta_{j_1 j_1'}\delta_{j_2 j_2'} - S_l(j_1 j_2; j_1' j_2')|^2 \ . \tag{35}$$

III. THE INTERACTION POTENTIAL FOR H_2-HD

The interaction potential between H_2 and HD is not available. However, the potential for H_2–H_2 should be appropriate also for H_2–HD, except that it must be expressed in terms of the coordinates of the center of mass of HD. The HD molecule is the simplest example of the so-called "loaded spheres." This type of molecule has an intermolecular force field that is spherically symmetric (or nearly so) about a center of force, but it has a large effective anisotropy due to eccentric rotation about a rotation axis which is appreciably displaced by about 0.123 Å towards the deuterium end of the molecule.

The H_2–H_2 interaction potential has been widely investigated both experimentally and theoretically.[23–26] In this study the H_2–H_2 potential we chose to use has the form

$$V(R', \theta_1', \theta_2') = V_0(R')[1 + \alpha P_2(\cos\theta_1') + \alpha P_2(\cos\theta_2')] \ , \tag{36}$$

where R', θ_1', and θ_2' are defined in Fig. 2 and $V_0(R')$ is the spherically symmetric potential determined experimentally by Farrar and Lee[26] using a molecular beam technique. The parameter α is the strength of anisotropy for which we adopt the value 0.14, that Davison[20,27] found necessary to fit the rotation relaxation times. This potential form [Eq. (36)] was also adopted by Zarur and Rabitz[6] in their studies of H_2–H_2 collisions. The potential should be a reasonable model for H_2–H_2 and therefore H_2–HD and should be able to exhibit the essential feature of H_2–HD collisions.

The potential [Eq. (36)] is now reexpanded in terms of the new coordinates (R, θ_1, θ_2) which are illustrated in Fig. 2. We have computed $V(R', \theta_1', \theta_2')$ for a grid of $R'\theta_1'\theta_2'$ points and fit it to a form like Eq. (4) as follows:

$$V_I(R, \theta_1, \theta_2) = v_{000}(R) + v_{200}(R)P_2(\cos\theta_1) + [v_{010}(R)P_1(\cos\theta_2) + v_{020}(R)P_2(\cos\theta_2) + v_{030}(R)P_3(\cos\theta_2)]$$

$$+ v_{210}(R)P_2(\cos\theta_1)P_1(\cos\theta_2) \ , \tag{37}$$

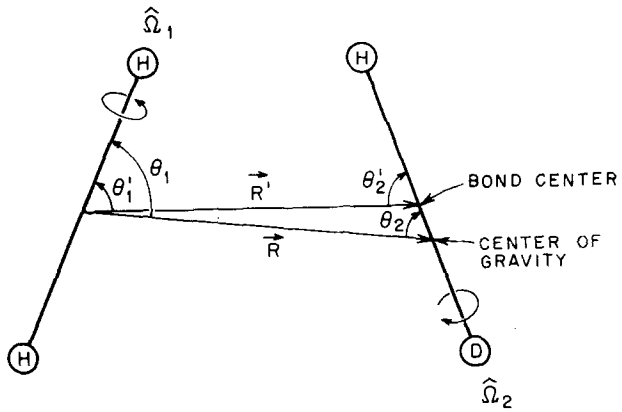

FIG. 2. Geometry of the H_2–HD collision system.

where $v_{l_1 l_2 l}(R)$ have the same meaning as those defined in Eq. (4). These radial potentials $v_{l_1 l_2 l}(R)$ are plotted in Figs. 3(a) and 3(b) as a function of intermolecular distance R. Higher angular terms with $l_1+l_2>3$ that have been ignored are at least an order of magnitude smaller and are of minor significance in scattering calculations.

Owing to vibronic interaction, the HD molecule possesses a permanent dipole moment in addition to its permanent quadrupole moment. Accordingly, we have also considered the quadrupole–dipole (V_{QD}) and the quadrupole–quadrupole (V_{QQ}) interactions between H_2 and HD. Thus, the full H_2–HD interaction potential adopted in our present calculations is

$$V_{II} = V_I + V_{QD} + V_{QQ} \ , \tag{38}$$

where

$$V_{QD} = v_{213}(R) \sum_{m_1 m_2 m} \langle 2m_1 1 m_2 | 213 m \rangle \times Y_{2m_1}(\hat{\Omega}_1) Y_{1m_2}(\hat{\Omega}_2) Y^*_{3m}(\hat{R}) \ , \tag{39}$$

and

$$V_{QQ} = v_{224}(R) \sum_{m_1 m_2 m} \langle 2m_1 2 m_2 | 224 m \rangle \times Y_{2m_1}(\hat{\Omega}_1) Y_{2m_2}(\hat{\Omega}_2) Y^*_{4m}(\hat{R}) \ , \tag{40}$$

with

$$v_{213}(R) = -(4\pi)^{3/2}(1/7)^{1/2} Q_1 \mu_2 / R^4 \tag{41}$$

and

$$v_{224}(R) = +(4\pi)^{3/2}(14/45)^{1/2} Q_1 Q_2 / R^5 \ . \tag{42}$$

Q_1, Q_2, and μ_2 are, respectively, the quadrupole moments of H_2 and HD and the dipole moment of HD. The $1/R^4$ radial dependence of the quadrupole–dipole term was smoothly cut off for $R \lesssim R_m$, where R_m is the position of the minimum in the $v_{000}(R)$ potential. This was accomplished by replacing $1/R^4$ by $[R+0.1(R_m/R)^{12}a_0]^{-4}$, which rapidly takes on the correct long-range behavior for $R \gtrsim R_m$. Similarly, the $1/R^5$ dependence of the quadrupole–quadrupole term was replaced by $[R+0.2(R_m/R)^{12}a_0]^{-5}$.

The potential V_{II} given in Eq. (38) was converted into effective potentials using the formulas of the previous section. The result is

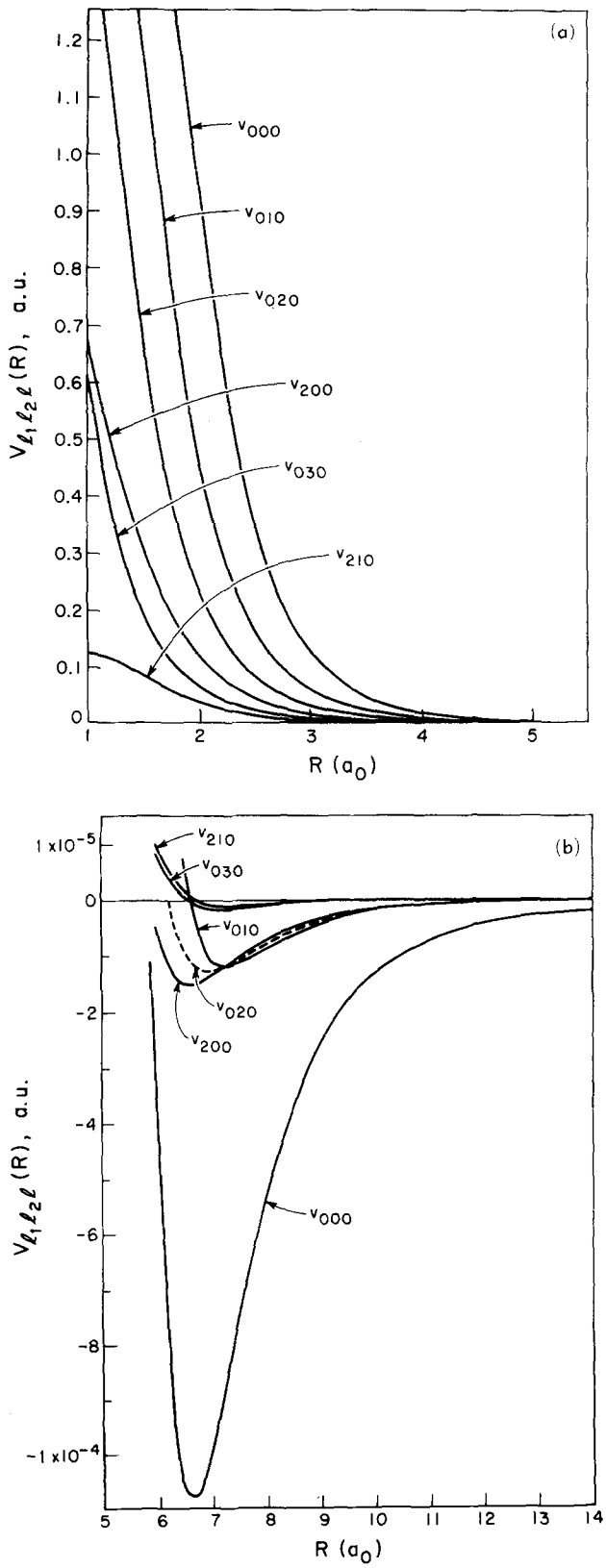

FIG. 3. (a) The short-range parts of potentials $v_{l_1 l_2 l}(R)$; (b) The potential wells and the long-range parts of $v_{l_1 l_2 l}(R)$.

$$\langle j_1 j_2 | V_{II}^{eff} | j_1' j_2' \rangle = v_{000}(R)\delta_{j_1 j_1'}\delta_{j_2 j_2'} + Ne^{in}\left\{A_{200}^{202}(R)\langle j_1 j_2 \| T_{202} \| j_1' j_2' \rangle + \sum_{\alpha=1}^{3} A_{0\alpha 0}^{0\alpha\alpha}(R)\langle j_1 j_2 \| T_{0\alpha\alpha} \| j_1' j_2' \rangle \right.$$

$$\left. + \sum_{\beta=1,3} A_{210}^{21\beta}(R)\langle j_1 j_2 \| T_{21\beta} \| j_1' j_2' \rangle + v_{213}(R)\langle j_1 j_2 \| T_{213} \| j_1' j_2' \rangle + v_{224}(R)\langle j_1 j_2 \| T_{224} \| j_1' j_2' \rangle \right\} . \quad (43)$$

IV. SCATTERING CALCULATIONS

The coupled differential equations, Eq. (28), with the effective potential matrix elements given by Eq. (43) were integrated with appropriate basis sets using the Numerov algorithm.[28] The resulting S-matrix elements are accurate to about three significant figures. The integral cross sections were calculated using Eq. (35).

The molecules were treated as rigid rotors with rotational constants $B_e = 59.3$ cm^{-1} for H_2 and $B_e = 44.7$ cm^{-1} for HD. The dipole[29] and quadrupole[24] moments for HD are, respectively, $2.3024\times10^{-4}\, ea_0$ and $0.477\, ea_0^2$ and the quadrupole moment[24] of H_2 is $0.490\, ea_0^2$, where a_0 is the Bohr radius.

We have tested the degree of convergence with respect to the size of the basis set. As an example, we compare in Table I the cross sections for transitions (00 → 01), (00 → 02), and (01 → 02), using two different basis sets. The first set includes only (00), (01), and (02) channels while the second one includes all the open channels (00), (01), (02), (20), and (21) at the specific energy $E = 0.0555$ eV. The inclusion of the two extra higher-lying channels (20) and (21) does not appear to have any appreciable effect on the lower-lying transitions. Thus, within the error that might be introduced by the uncertainty of the interaction potential, it is adequate to include only all the open channels in the scattering calculations.

V. RESULTS AND DISCUSSION

In this section, we shall present and discuss the results for the inelastic integral cross sections. As far as astrophysical application is concerned, we are particularly interested in the pure rotational transitions of HD. Simultaneous excitations of both H_2 and HD are less probable at low energy collisions and the corresponding inelastic cross sections are much smaller than those of pure HD transitions. We shall accordingly be concerned mainly with the following family of excitation cross sections of HD;

$$H_2(j_1) + HD(j_2) \rightarrow H_2(j_1' = j_1) + HD(j_2 \neq j_2') \quad . \quad (44)$$

The integral cross sections for pure HD transitions are depicted in Figs. 4–6 for the specific member $j_1 = j_1' = 0$, with $\Delta j_2 = j_2' - j_2 = +1$, $+2$, and $+3$. All the transitions exhibit a similar behavior with energy: the cross sections rise rapidly for energies close to the threshold and continue to increase smoothly, though less rapidly, with increasing impact energy. A similar behavior occurs for other members of the pure HD transitions with $j_1 = j_1' \neq 0$, where j_1 can be even (para-H_2) or odd (ortho-H_2).

We have examined the ratios $\sigma(j_1 \neq 0, j_2 \rightarrow j_1' = j_1, j_2')/\sigma(j_1 = 0, j_2 \rightarrow j_1' = 0, j_2')$ for various transitions and found that they are usually not equal to unity but deviate from unity by 5% to 20%. These discrepancies are primarily due to the fact that different transitions can be coupled by different parts of the interaction potential. To understand the sensitivity of the various transitions to the potential, we compare $\sigma(00 \rightarrow 01)$ and $\sigma(10 \rightarrow 11)$ in Table II. The set of cross sections with superscript index a or b are obtained with or without, respectively, the quadrupole–dipole interaction V_{QD}. It is interesting to note that

$$\sigma(00 \rightarrow 01)^a \approx \sigma(00 \rightarrow 01)^b \quad (45a)$$

and

$$\sigma(10 \rightarrow 11)^a \approx \sigma(10 \rightarrow 11)^b \quad . \quad (45b)$$

The relation (45a) is easily understood because the transition (00 → 01) is not coupled by V_{QD}. The transition (10 → 11), however, is coupled by V_{QD}. Thus, the equality (45b) simply implies that V_{QD} is too small to appreciably affect the $|\Delta j_2| = 1$ transitions, in accord with the fact that the dipole moment of HD is negligibly small. We next compare $\sigma(10 \rightarrow 11)$ and $\sigma(00 \rightarrow 01)$ as a function of collision impact energy. We found that $\sigma(10 \rightarrow 11)$ is less than $\sigma(00 \rightarrow 01)$ at lower energies, but the reverse is true for $E \gtrsim 0.025$ eV. This phenomenon cannot be attributed to any simple physical cause but arises from several interferring factors. In Table III A. and B., the nonzero coupling coefficients $F_{l_1 l_{2I}}(j_1 j_2 \rightarrow j_1' j_2')$ associated with radial potentials $v_{l_1 l_{2I}}(R)$ for transitions $(j_1 j_2 \rightarrow j_1' j_2')$ are listed. We first note that although three terms v_{010}, v_{210}, and v_{213} contribute to the (10 → 11) transition, only a single v_{010} term contributes to the (00 → 01) transition. Owing to its smallness, the term v_{213}, of course, can be simply ignored here. The coupling coefficients F_{010} and F_{210} are, however, different in sign. Thus, the net contribution to the (10 → 11) transition is due to the cancellation of the $v_{010}(R)$ F_{010} and $v_{210}(R)$ F_{210} effective interactions. This explains why (10 → 11) is smaller than $\sigma(00 \rightarrow 01)$ at low energies. As the energy becomes higher, the short-range part of $v_{010}(R)$ increases more rapidly than that of $v_{210}(R)$ and becomes the dominant term for causing

TABLE I. Comparison of excitation cross sections for different basis sets. $E = 0.0555$ eV.

Transitions $j_1 j_2 \rightarrow j_1' j_2'$	Basis set (00), (01), (02)	Basis set (00), (01), (02), (20), (21)
00 → 01	22.86[a]	22.84
00 → 02	1.27	1.27
01 → 02	7.22	7.22

[a]Cross sections are in units of a_0^2.

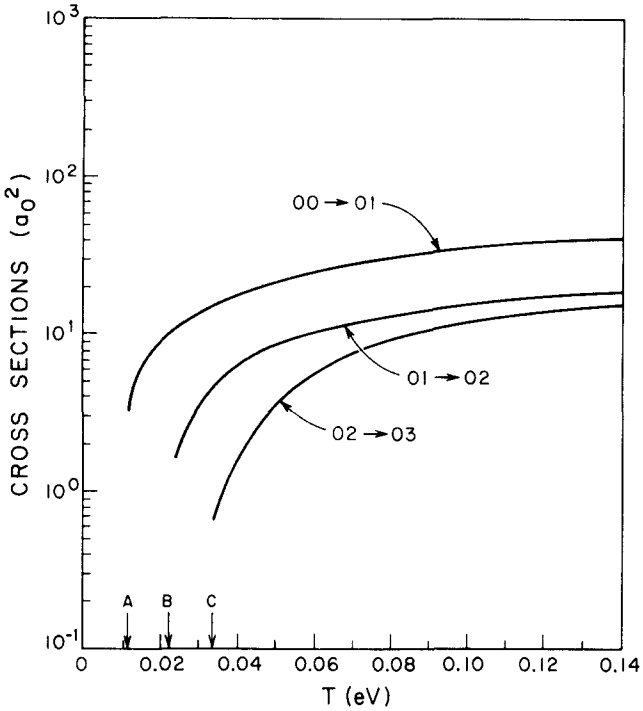

FIG. 4. Calculated cross sections for rotational excitation of HD by collisions with H_2 as a function of relative kinetic energy T with $\Delta j_1 = 0$ and $\Delta j_2 = +1$. A, B, and C represent, respectively, the threshold energy for the transitions (00 → 01), (01 → 02), and (02 → 03).

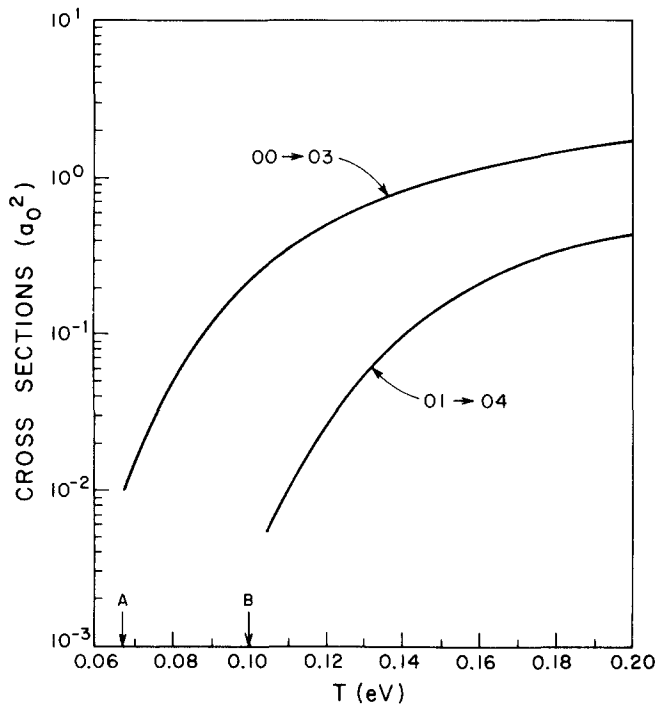

FIG. 6. Calculated cross sections for rotational excitation of HD by collisions with H_2 as a function of relative kinetic energy T with $\Delta j_1 = 0$ and $\Delta j_2 = +3$. A and B are, respectively, the threshold energy for the (00 → 03) and (01 → 04) transitions.

$\Delta j_2 = 1$ transition [cf. Fig. 3(a)]. Thus, the cancellation between $v_{010} F_{010}$ and $v_{210} F_{210}$ becomes less effective and $\sigma(10 \rightarrow 11)$ should approach $\sigma(00 \rightarrow 01)$ eventually. However, at higher energies, $\sigma(10 \rightarrow 11)$ is larger than $\sigma(00 \rightarrow 01)$ and the cancellation effect alone does not explain the observations. We now compare Table III a and b more carefully and notice that there is no nonzero diagonal coupling coefficient in the (00 → 00) transition, whereas there is one term, F_{200}, that survives in the diagonal (10 → 10) transition. Recall now that the degree of anisotropy is meaningful only in relation to the magnitude of the spherically symmetric part of the potential.[30] In other words, although the spherically symmetric part of the potential is primarily responsible for the elastic cross section, it also plays an essential role in the inelasticity because it can act as a shield for the anisotropic part of the potential. When we speak of the "spherically symmetric part" of the potential, we should include both the physical spher-

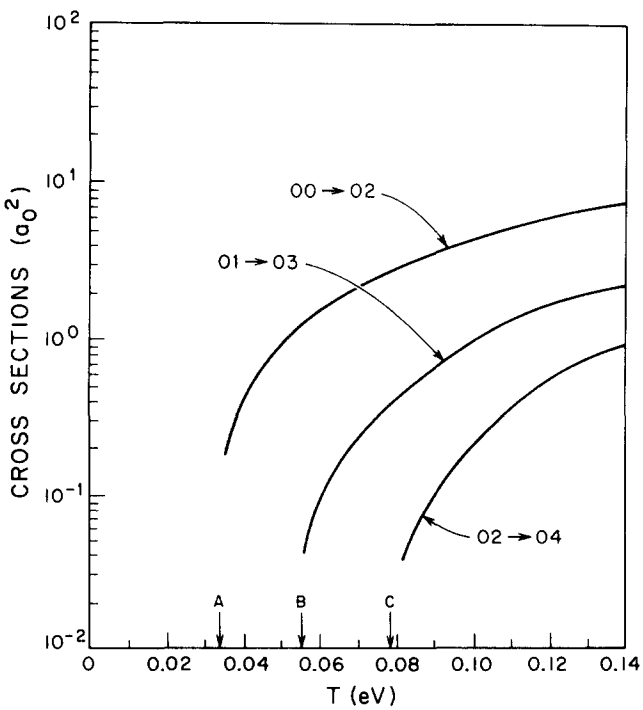

FIG. 5. Calculated cross sections for rotational excitation of HD by collisions with H_2 as a function of relative kinetic energy T with $\Delta j_1 = 0$ and $\Delta j_2 = +2$. A, B, and C denote, respectively, the threshold energy for the transitions (00 → 02), (01 → 03), and (02 → 04).

TABLE II. Comparison of $\Delta j_1 = 0$, $\Delta j_2 = 1$ transitions from HD colliding with para-H_2- and ortho-H_2. Cross sections are in units of a_0^2 and T is the intial relative kinetic energy in eV.

T \ $j_1 j_2 \rightarrow j_1' j_2'$	(00 → 01)[a]	(00 → 01)[b]	(10 → 11)[a]	(10 → 11)[b]
0.0115	3.42	3.42	3.11	3.11
0.0150	6.18	•••	6.08	•••
0.0250	11.54	11.55	11.95	11.95
0.0450	19.33	•••	20.86	•••
0.0555	22.84	22.82	24.75	24.76
0.0670	26.57	•••	27.62	•••
0.0750	28.69	•••	30.94	•••

[a] V_{QD} is included in scattering calculations.
[b] V_{QD} is deleted in scattering calculations.

TABLE III. Nonzero coupling coefficients $F_{l_1l_2l}(j_1j_2 \to j_1'j_2')$ associated with radial potentials $v_{l_1l_2l}(R)$ for transitions $j_1j_2 \to j_1'j_2'$.

A. ortho-H_2

j_1j_2 \ $j_1'j_2'$	(1,0)	(1,1)	(1,2)
(1,0)	$F_{200}(-)$[a]	$F_{010}(+), F_{210}(-)$ $F_{213}(-)$	$F_{020}(+)$, $F_{224}(-)$
(1,1)		$F_{200}(-)$, $F_{020}(-)$ $F_{224}(+)$	$F_{010}(+)$, $F_{030}(-)$ $F_{210}(-)$, $F_{213}(-)$
(1,2)			$F_{200}(-)$, $F_{020}(-)$ $F_{224}(+)$

B. para-H_2

j_1j_2 \ $j_1'j_2'$	(0,0)	(0,1)	(0,2)
(0,0)	none	$F_{010}(+)$[a]	$F_{020}(+)$
(0,1)		$F_{020}(-)$	$F_{010}(+)$, $F_{030}(-)$
(0,2)			$F_{020}(-)$

[a]The symbol (+ or −) in parentheses indicates the sign of the coupling coefficient for that particular transition specified by $(j_1j_2) \to (j_1'j_2')$.

ically symmetric potential $v_{000}(R)$ as well as the anisotropic potential corresponding to the relevant diagonal (elastic) transitions. Thus, for the (10 → 11) transition, the degree of anisotropy should be measured by the effective cancellation, $F_{010}v_{010}(R) - |F_{210}|v_{210}(R)$, with respect to the "effectively" spherically symmetric part, namely, $v_{000}(R)+F_{200}v_{200}(R)$. On the other hand, the anisotropy of the (00 → 01) transition is measured only by the single $v_{010}(R)F_{010}$ term with respect to $v_{000}(R)$. However, since the sign of F_{200} is negative, the effectively spherically symmetric part of the potential is thereby smaller for the (10 → 11) transition than for the (00 → 01) transition. Thus, it is not surprising that in some energy regions the effective anisotropy for the (10 → 11) is larger than that for the (00 → 01) transition.

The (00 → 02) and (10 → 12) transitions are compared in Table IV. The superscript a or b indicates that the associated transition is calculated with or without the quadrupole–quadrupole interaction V_{QQ} included. We notice that

TABLE IV. Comparison of $\Delta j_1 = 0$, $\Delta j_2 = 2$ transitions for HD colliding with para-H_2 and ortho-H_2. Cross sections are in units of a_0^2 and T is the initial relative kinetic energy in eV.

T \ $j_1j_2 \to j_1'j_2'$	(00 → 02)[a]	(00 → 02)[b]	(10 → 12)[a]	(10 → 12)[b]
0.035	0.19	0.19	0.18	0.20
0.045	0.66	0.66	0.68	0.72
0.0555	1.27	...	1.34	...
0.075	2.55	2.55	2.72	2.81
0.115	5.48	...	6.02	...

[a]V_{QQ} is included in scattering calculations.
[b]V_{QQ} is deleted in scattering calculations.

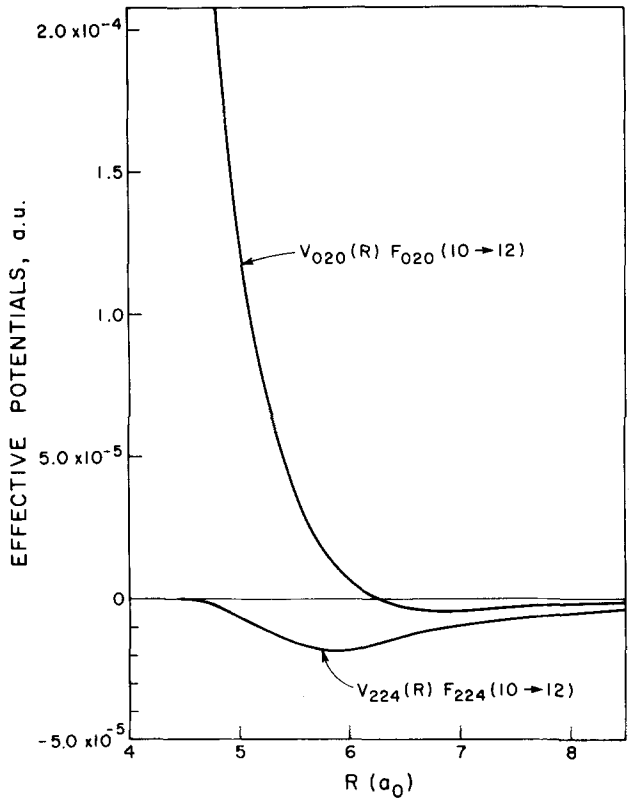

FIG. 7. Comparison of the effective interactions $v_{020}(R)F_{020}$ and $v_{224}(R)F_{224}$ for the transition $H_2(j_1=1)+HD(j_2=0) \to H_2(j_1'=1)+HD(j_2'=2)$.

(a) $\sigma(00 \to 02)^a \approx \sigma(00 \to 02)^b$, (46a)

(b) $\sigma(10 \to 12)^a < \sigma(10 \to 12)^b$, (46b)

and the ratio $\sigma(10 \to 12)^a/\sigma(10 \to 12)^b$ deviates from unity by 10% at $T = 0.035$ eV and drops to only 3.2% at $T = 0.075$ eV.

(c) The ratio $\sigma(10 \to 12)^a/\sigma(00 \to 02)^a$ is an increasing function of energy. It is less than unity for $T \lesssim 0.035$ eV and becomes greater than unity for $T \gtrsim 0.045$ eV.

The relation (46a) is apparently due to the fact that the (00 → 02) transition is not coupled by the V_{QQ} interaction. However, the (10 → 12) transition is coupled by V_{QQ} and the difference between $\sigma(10 \to 12)^a$ and $\sigma(10 \to 12)^b$ reflects the effect of V_{QQ}. The ratio $\sigma(10 \to 12)^a/\sigma(10 \to 12)^b$ approaches unity rapidly as the impact energy becomes higher, and V_{QQ} is more effective at lower energy than at higher energy. This is because the V_{QQ} interaction is a weak, long-range interaction, and as T increases, the molecules tend to sample more and more of the short-range $P_2(\cos\theta_2)$ type of anisotropy. However, the relation (46b) implies that the transition $\sigma(10 \to 12)$ is decreased by the presence of the Q–Q term, a fact which is opposite to that Zarur and Rabitz[6] had observed in their H_2–H_2 studies. There is actually no contradiction between these two observations. The (10 → 12) transition is induced by both the $v_{020}(R)F_2(\cos\theta_2)$ and the V_{QQ} interactions. In Fig. 7, the effective interactions $v_{020}(R)F_{020}(10 \to 12)$ and $v_{224}(R)F_{224}(10 \to 12)$ are compared. Here F_{020} and F_{224} are the coupling coef-

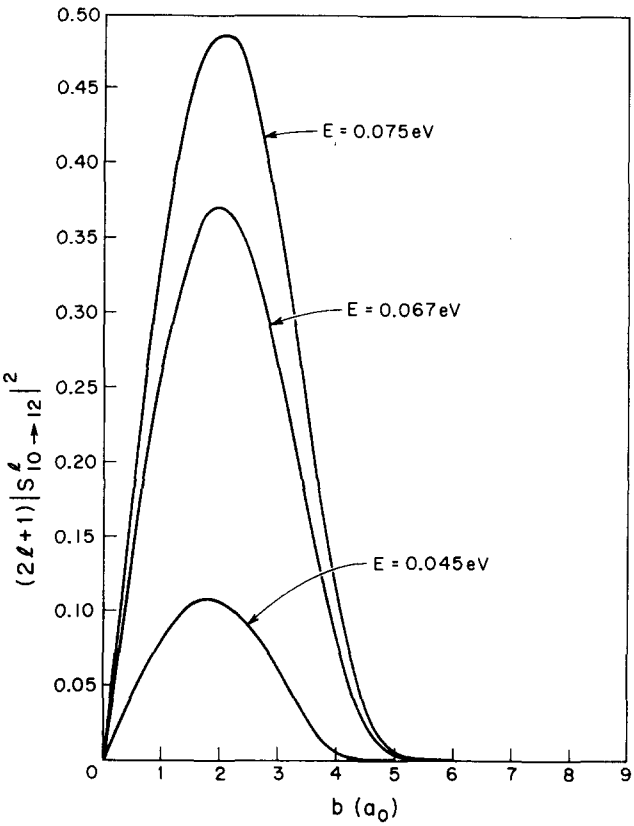

FIG. 8. Variation of the quantity $(2l+1)\,|s^l_{10\to12}|^2$ with impact parameter b for three different collision energies.

ficients associated with the potentials $v_{020}(R)$ and $v_{224}(R)$ (the Q–Q radial part). Since these two effective interactions are opposite in sign for distances most effective in causing transitions ($R < 6.2\,a_0$), there is an effective cancellation between them. As a result, the excitation cross sections are decreased by the presence of the Q–Q interaction.

Finally, we analyze the observation (c). Here we first notice that $\sigma(10\to12)^a$ is smaller than $\sigma(00\to02)^a$ at the low energy region, $E \lesssim 0.035$ eV. This is clearly due to the negative contribution from the presence of the Q–Q interaction. However, as energy increases, $\sigma(10\to12)^a$ becomes increasingly larger than $\sigma(00\to02)^a$. This phenomenon cannot be explained by the effect of the Q–Q term, because the latter diminishes with increasing energy. It can be explained, however, by the concept of effective anisotropy measured with respect to the effective spherically symmetric part of the potential as we discussed for the $\Delta j_2 = 1$ transitions.

From Fig. 7, we observe that the attractive long-range part of $v_{020}(R)$ is about an order of magnitude smaller than that of $v_{QQ}(R)$. However, the effect of the Q–Q interaction is not large. Even at the lowest energy shown in Table IV, the presence of the Q–Q interaction changes the cross section $\sigma(10\to12)$ by only 10%. This immediately suggests that it is the short-range anisotropic part of the potential that mainly controls the rotational excitation. To elucidate the point more clearly, we show in Fig. 8 the quantity $(2l+1)\,|S^l_{10\to12}|^2$ as a function of impact parameter b, the latter being calcu-

TABLE V. Collisional rate constants $R_{j_2 j_2'}$ (10^{-10} cm^3 sec^{-1}).

A. $H_2(j_1=0) + HD(j_2) \to H_2(j_1'=0) + HD(j_2'=j_2+1)$.

T(°K) \ $R_{j_2 j_2'}$	R_{01}	R_{12}	R_{23}	R_{34}
5	2.21-12[a]	6.10-25	4.24-35	7.08-50
10	1.11-6	5.44-13	3.58-18	1.64-25
20	7.91-4	4.91-7	1.01-9	2.35-13
30	7.32-3	4.83-5	6.82-7	2.64-9
40	2.30-2	4.91-4	1.83-5	2.86-7
50	4.72-2	2.01-3	1.35-4	4.84-6
60	7.76-2	5.28-3	5.28-4	3.25-5
80	1.51-1	1.82-2	3.03-3	3.66-4
100	2.35-1	3.96-2	9.08-3	1.63-3
150	4.69-1	1.21-1	4.35-2	1.32-2
200	7.21-1	2.26-1	1.03-1	4.07-2
300	1.24	4.64-1	2.70-1	1.37-1
400	1.76	7.04-1	4.64-1	2.65-1
500	2.27	9.33-1	6.61-1	4.00-1
600	2.75	1.14	8.50-1	5.33-1
700	3.20	1.34	1.02	6.59-1
800	3.62	1.52	1.19	7.77-1

B. $H_2(j_1=0) + HD(j_2) \to H_2(j_1'=0) + HD(j_2'=j_2+2)$.

T(°K) \ $R_{j_2 j_2'}$	R_{02}	R_{13}	R_{24}
5	7.55-37[a]	2.18-58	2.37-84
10	2.58-19	2.67-30	3.04-43
20	1.46-10	2.90-16	1.03-22
30	1.23-7	1.42-11	7.23-16
40	3.72-6	3.24-9	1.96-12
50	2.96-5	8.67-8	2.31-10
60	1.21-4	7.93-7	5.68-9
80	7.43-4	1.34-5	3.29-7
100	2.33-3	7.80-5	3.98-6
150	1.22-2	9.65-4	1.27-4
200	3.17-2	3.87-3	8.00-4
300	9.67-2	1.82-2	5.63-3
400	1.88-1	4.29-2	1.57-2
500	2.96-1	7.43-2	2.96-2
600	4.11-1	1.08-1	4.55-2
700	5.27-1	1.44-1	6.21-2
800	6.41-1	1.79-1	7.87-2

C. $H_2(j_1=0) + HD(j_2) \to H_2(j_1'=0) + HD(j_2'=j_2+3 \text{ or } 4)$.

T(°K) \ $R_{j_2 j_2'}$	R_{03}	R_{14}	R_{04}
5	4.37-70[a]	2.06-107	4.80-119
10	2.05-36	3.81-55	3.38-61
20	1.38-19	4.92-29	2.69-32
30	5.86-14	2.51-20	1.17-22
40	3.99-11	5.82-16	7.96-18
50	2.08-9	2.49-13	6.51-15
60	3.02-8	1.45-11	5.86-13
80	9.23-7	2.50-9	1.74-10
100	7.75-6	5.86-8	5.74-9
150	1.59-4	4.63-6	7.34-7
200	8.34-4	4.67-5	9.60-6
300	5.27-3	5.34-4	1.43-4
400	1.47-2	1.89-3	5.85-4
500	2.83-2	4.12-3	1.37-3
600	4.48-2	6.97-3	2.45-3
700	6.27-2	1.01-2	3.70-3
800	8.11-2	1.35-2	5.06-3

[a]Powers of ten.

TABLE VI. Calculated rotational relaxation times for H_2–HD system.

Temperature (°K)	τ_{rot} (10^{-10} sec/atm)
10	0.97
20	1.67
30	2.22
40	2.55
50	2.70
60	2.75
70	2.74
80	2.71
90	2.67
100	2.62

lated by the usual expression

$$b = \hbar(l+\tfrac{1}{2})/\mu v \ ,$$

where l is the orbital angular momentum, μ is the reduced mass of H_2–HD, and v is the relative collision velocity. From a semiclassical point of view, the quantity $|S^l_{10\to12}|^2$ is equivalent to the semiclassical transition probability as a function of impact parameters,

$$|S^l_{10\to12}|^2 \approx P_{10\to12}(b) \ ,$$

and $(2l+1)|S^l_{10\to12}|^2$ is equivalent to $2bP(b)$. The transition probabilities decrease rather rapidly with decreasing collision energy but the range of impact parameters that contributes to the transition remains approximately unchanged. In particular, the most probable impact parameter occurs for $1.5\,a_0 < b < 3.0\,a_0$; the probabilities approach zero beyond $6\,a_0$.

VI. RATE CONSTANTS FOR ROTATIONAL EXCITATION OF HD BY COLLISIONS WITH H_2

The Maxwellian-averaged rate constants for the transition

$$H_2(j_1) + HD(j_2) \to H_2(j_1') + HD(j_2')$$

are given by the expression

$$R(j_1 j_2 \to j_1' j_2') = \left(\frac{8kT}{\pi\mu}\right)^{1/2} \frac{1}{(kT)^2} \times \int_0^\infty E \exp(-E/kT)\,\sigma(j_1 j_2 \to j_1' j_2'|E)\,dE \ , \tag{47}$$

where μ is the reduced mass for H_2–HD, k is the Boltzmann constant, E is the initial relative kinetic energy, and $\sigma(E)$ is the inelastic cross section corresponding to the specific collision energy E. We present the results in Table VA.–C. for the pure rotational excitations of HD caused by para-H_2. The corresponding rate constants for HD+ortho-H_2 collisions are about 5%–20% larger and will not be shown here. The deexcitation rate constants can be easily calculated through the detailed-balance relationship.

These rate constants for the rotational excitation of HD by H_2 are critical parameters in the evaluation of the cooling of interstellar clouds by HD. Research along this direction is now underway.

VII. ROTATIONAL RELAXATION OF HD

Experiments that measure the relaxation of internal states of molecules through collisional energy transfer are susceptible to theoretical analysis in terms of an assumed interaction potential. Comparisons of experimental and theoretical results then provide the criteria necessary to evaluate the validity of the potential.

The sound absorption experiment which measures the rotational relaxation time is an important means of studying rotational inelastic collisions. For a two-level system, the roational relaxation time τ_{rot} is related to the rotationally inelastic cross sections by the relation[31]

$$\tau_{rot}^{-1} = N\langle v\rangle[\langle\sigma_{1\to2}\rangle + \langle\sigma_{2\to1}\rangle] \ . \tag{48}$$

Here N is the number density, $\langle v\rangle = (8kT/\pi\mu)^{1/2}$ is the average relative velocity, and $\langle\sigma_{jj'}\rangle$ is the Maxwellian averaged cross section for rotational transition from level j to level j'.

For the HD molecule at temperatures below 150 °K, only the lowest two rotational levels are significantly populated, and its corresponding rotational relaxation time can be computed by

$$\tau_{rot}^{-1} = N[R(j_1=0, j_2=0 \to j_1'=0, j_2'=1) + R(j_1=0, j_2=1 \to j_1'=0, j_2'=0)] \ , \tag{49}$$

or

$$\tau_{rot} = \frac{kT}{P}\{[1+\tfrac{1}{3}\exp(2B/kT)] \times R(j_1=0, j_2=0 \to j_1'=0, j_2'=1)\}^{-1} \ , \tag{50}$$

where P is the gas pressure, B is the rotational constant of HD, and $R(j_1=0,\ j_2=0 \to j_1'=0,\ j_2'=1)$ is the rate constant for the transition

$$H_2(j_1=0) + HD(j_2=0) \to H_2(j_1'=0) + HD(j_2'=1) \ .$$

We have calculated the rotational relaxation time for the lowest two levels of HD at 1 atm. The results are presented in Table VI in the temperature range from 5–100 °K. Prangsma *et al.*[16] have recently made sound absorption measurements for pure HD, HD+He, and HD+Ne. Their experimentally determined rotational relaxation times for the HD–He system are quite close to our theoretical values for the HD–H_2 system. The interaction potentials for the HD–He and HD–H_2 systems should be similar though the latter system probably possesses a larger anisotropy. Future experimental work on the rotational relaxation times of HD–H_2 system would be useful in assessing and improving the reliability of the present HD–H_2 interaction potential, especially the repulsive anisotropic part.

ACKNOWLEDGMENTS

This research was supported by the National Science Foundation under contract No. GP-39308X. The author is indebted to Professor A. Dalgarno for critical reading and suggestions on the preliminary manuscript. He is also grateful to Professor W. Reinhardt and Professor H. Rabitz for their comments.

[1]H. Rabitz, J. Chem. Phys. **57**, 1718 (1972).
[2]R. T. Pack, J. Chem. Phys. **60**, 633 (1974).
[3]P. McGuire and D. J. Kouri, J. Chem. Phys. **60**, 2488 (1974).
[4]S. -I Chu and A. Dalgarno, Proc. R. Soc. A **342**, 191 (1975).
[5]G. Zarur and H. Rabitz, J. Chem. Phys. **59**, 943 (1973).
[6]G. Zarur and H. Rabitz, J. Chem. Phys. **60**, 2057 (1974).
[7]S. -I Chu and A. Dalgarno, Astrophys. J. (submitted).
[8]H. Rabitz and G. Zarur, J. Chem. Phys. **61**, 5076 (1974).
[9]M. H. Alexander, J. Chem. Phys. **61**, 5167 (1974).
[10]S. -I Chu (unpublished results).
[11]S. Green, J. Chem. Phys. (submitted).
[12]S. -I Chu and A. Dalgarno, J. Chem. Phys. (submitted).
[13]S. Green and P. Thaddeus, Astrophys. J. (submitted).
[14]Y. Itikawa and K. Takayanagi, J. Phys. Soc. Jpn. **32**, 1605 (1972).
[15]S. Green, Physica (Utr.) (submitted).
[16]G. J. Prangsma, J. P. J. Heemskerk, H. F. P. Knaap, and J. J. M. Beenakker, Physica (Utr.) **50**, 433 (1970).
[17]K. Takayanagi, Sci. Rep. Saitama Univ. A **3**, 87 (1959); K. Takayanagi, ISAS Report No. 467, Univ. Of Tokyo, 1971.
[18]A. Dalgarno and E. L. Wright, Astrophys. J. Lett. **174**, L49 (1972).
[19]C. G. Gray, Can. J. Phys. **46**, 135 (1968).
[20]W. D. Davison, Discuss. Faraday Soc. **33**, 71 (1962).
[21]D. M. Brink and G. R. Satchler, *Angular Momentum* (Clarendon, Oxford, England, 1968), 2nd ed.
[22]We thank Professor H. Rabitz for pointing out to us his recent paper, M. R. Verter and H. Rabitz, J. Chem. Phys. **61**, 3707 (1974), in which a similar relation is given between body-fixed and space-fixed potentials for two symmetric tops.
[23]See the following review article for detailed references: A. K. McMahan, H. Beck, and J. A. Krumhansi, Phys. Rev. A **9**, 1852 (1974).
[24]D. Stogryn and A. Stogryn, Mol. Phys. **11**, 371 (1966).
[25]P. W. Langhoff, R. Gordon, and M. Karplus, J. Chem. Phys. **55**, 2126 (1971).
[26]J. M. Farrar and Y. T. Lee, J. Chem. Phys. **57**, 5492 (1972).
[27]W. D. Davison, Proc. R. Soc. A **280**, 227 (1964).
[28]A. C. Allison, J. Comput. Phys. **6**, 378 (1970).
[29]M. Trefler and H. P. Gush, Phys. Rev. Lett. **20**, 703 (1968).
[30]G. Wolken, W. H. Miller, and M. Karplus, J. Chem. Phys. **56**, 4930 (1972).
[31]R. Shafer and R. G. Gordon, J. Chem. Phys. **58**, 5422 (1973).